International Journal of Pharmaceutics 360 (2008) 197–203

Contents lists available at ScienceDirect

International Journal of Pharmaceutics

journal homepage: www.elsevier.com/locate/ijpharm

Pharmaceutical Nanotechnology

# Asialoglycoprotein receptor-targeted superparamagnetic iron oxide nanoparticles

Guifang Huang[a,1], James Diakur[a,2], Zhenghe Xu[b], Leonard I. Wiebe[a,c,*]

[a] Faculty of Pharmacy and Pharmaceutical Sciences, Edmonton, Canada
[b] Faculty of Engineering, University of Alberta, Edmonton, Canada
[c] Cross Cancer Institute, 1807 PET Centre, 11560 University Avenue, Edmonton, AB T6B 1Z2, Canada

ARTICLE INFO

*Article history:*
Received 23 October 2007
Received in revised form 14 April 2008
Accepted 15 April 2008
Available online 26 April 2008

*Keywords:*
Superparamagnetic iron oxide (SPIO) nanoparticles
Asialoglycoprotein receptor (ASPGR)
Drug targeting
Amino-functionalized SPIO
Galactose-terminal ASPIO

ABSTRACT

Superparamagnetic iron oxide (SPIO) nanoparticles are primarily used as contrast agents in magnetic resonance imaging. SPIO have also been derivatized to add targeting and drug-carrier functionality as drug delivery devices. The preparation and characterization of amino-functionalized SPIO (ASPIO) and lactose-derivatized galactose-terminal-ASPIO are now reported. The target for galactose-terminal-ASPIO is the cell-surface asialoglycoprotein receptor (ASGPR) expressed by hepatocytes. Two batches of ASPIO with average particle sizes of 61 [42] nm and 127 [125] nm [full-width half maximum; FWHM] were prepared. The small ASPIO increased from 61 nm to 278 [309] nm upon lactosylation (Gal-ASPIO-278) and to 302 [280] by *N*-acetylation (NAcASPIO-302); the larger ASPIO afforded galactosyl-terminal ASPIO of 337 [372] nm and *N*-acetylated ASPIO of 326 [308] nm. The $LD_{50}$ of Gal-ASPIO-278 was 1500 μg/mL to HepG2 cells; Gal-ASPIO-278 associated with HepG2 cells in vitro, whereas NAcSPIO-302, prepared from the same ASPIO batch, did not. Gal-ASPIO-278 and NAcASPIO-302 were not bound by ASPGR non-expressing 143B cells. The association of Gal-ASPIO-278 to HepG2 cells was reduced by free galactose, supporting the model of ASGPR-mediated binding. These data underline the potential application of Gal-ASPIO as a targeted ligand for ASPGR-expressing cells in vivo.



## 1. Introduction

There are numerous established and potential applications for superparamagnetic nanoparticles (SPIO) in medicine and industry. In medicine, major interests relate to their potential as drug delivery devices and as contrast agents in magnetic resonance imaging (MRI) (Bulte and Kraitchman, 2004; Corot et al., 2006; Silva et al., 2007a).

Key developments in the preparation of enhanced SPIO involve the introduction of surface charge and/or surface coatings. This has been achieved primarily through electrostatic effects using citric (Wagner et al., 2002), 2,3-dimercaptosuccinic (Brillet et al., 2005) or oleic acids (Okassa et al., 2007). Dextran (Jung, 1995; Jung and Jacobs, 1995), poly(vinylalcohol phosphate) (Mohapatra et al., 2006), poly-epsilon caprolactone (Hamoudeh and Fessi, 2006) and silica/silanes (Liang et al., 2007; Zhang et al., 2007) have also been used to create polymer-coated SPIO. In addition, SPIOs have been prepared by polymerization using *N*-isopropylacrylamide (NIPAM) as the main monomer, methylene-bis-acrylamide as crosslinker and potassium persulfate as initiator (Shamim et al., 2007). Emulsification in organic solvents containing sorbitan tristerate with terephthaloyl chloride solution to attain interfacial cross-linking has also proven effective (Silva et al., 2007b). Polymeric surface coats may be functional in themselves through their influence on particle size and in vivo properties, or serve as platforms for the introduction of bioactive moieties such as cell-surface ligands of E-selectin (Boutry et al., 2006). In addition, SPIO have been encapsulated within large unilamellar vesicles of egg phosphatidylcholine and distearoyl-*SN*-glycero-3-phosphoethanolamine-*N*-[methoxy(poly-(ethyleneglycol))-2000] by film hydration and extrusion (Martina et al., 2005).

Charged functional groups were first introduced by chemical methods in which SPIO are treated with epichlorhydrin and ammonia (Palmacci and Josephson, 1993; Josephson et al., 1999). Cationic SPIOs have also been prepared by coating SPIOs with a silane coupling agent such as [*N*-(2-aminoethyl)-3-aminopropyl]trimethoxysilane (Liang et al., 2007; Zhang et al., 2007) to introduce amine functionality. In either case, the amino

* Corresponding author. Tel.: +1 780 979 4314; fax: +1 780 435 0636.
*E-mail address:* lenwiebe@cancerboard.ab.ca (L.I. Wiebe).
[1] Current address: Edmonton Radiopharmacy Centre, 11560 University Avenue, Edmonton, AB, Canada T6B 1Z2.
[2] Current address: Canam Bioresearch Inc., 6-1200 Waverly Street, Winnipeg, MB, Canada R3T 0P4.

0378-5173/$ – see front matter © 2008 Elsevier B.V. All rights reserved.
doi:10.1016/j.ijpharm.2008.04.029

groups provide a convenient anchor for proteins such as Annexin V (Smith et al., 2007), monoclonal antibodies (Liang et al., 2007), HIV-1 tat peptide (Zhao et al., 2002; Nitin et al., 2004) and trypsin (Li et al., 2007).

Effective targeting of selective tissue markers has been demonstrated using derivatized SPIO. For example, Annexin V-SPIO successfully targeted atherosclerotic plaque (Smith et al., 2007), Hepama-1 (humanized monoclonal antibody)-SPIO targeted liver cancer (Liang et al., 2007) and HIV-1 tat peptide-SPOI have demonstrated efficacy for intracellular magnetic labeling and non-invasive tracking of a large number of cell types (Zhao et al., 2002).

The asialoglycoprotein receptor (ASGPR) is a well-characterized molecular target expressed on the cell surface of hepatocytes and hepatomas (Morell et al., 1968; Kim et al., 2007; Li et al., in press). Asialorosomucoid (ASOR)-galactose-terminal protein derived from human $\alpha_1$-acid glycoprotein, and galactose-derivatized complexes, can be targeted specifically to hepatocytes by ASGPR on cell surfaces. Once complexed to the ASGPR, they enter the cell via ASGPR-mediated endocytosis (Wu et al., 2002).

The preparation and properties of galactose-derivatized superparamagnetic nanoparticles, and their in vitro uptake by ASGPR-expressing HepG2 cells, are now reported. The long-term goals of this approach are to assist in magnetic separation of hepatocyte cells in vitro, for use as cell markers for cell tracking, and for contrast enhancement in the diagnosis of liver disease using MRI.

## 2. Experimental

### 2.1. Materials

Lactose monohydrate, calcium chloride, sulfuric acid, potassium carbonate anhydrous, sodium chloride, sodium iodide, dibasic sodium phosphate, monobasic sodium phosphate, dimethyl sulfoxide and ammonium persulfate were purchased from BDH Inc., Canada. Acetic anhydride, methanol, sodium hydroxide, chloroform, ammonium hydroxide and HPLC water were purchased from Caledon Laboratories Ltd., Canada. Sodium cyanoborohydride, phenol, resorcinol, copper sulfate, isoamyl alcohol, sodium metabisulfite, galactose, mannose and 3-aminopropyltriethoxysilane [3-APTES, $NH_2$–$(CH_2)_3$–Si–$(CH_3CH_2O)_3$, 99%] were purchased from Aldrich Chemical Company Inc., USA. Hydrochloric acid was purchased from EM Science, an Associate of Merck Germany. Maghemite ($\gamma$-$Fe_2O_3$, 99+%) was provided by Alpha Chemicals, USA. EDTA, Tris base (Tris [hydroxymethy1] aminomethane), MTT (3-[4,5-dimethylthiazol-2yl]-2,5-diphenyl-tetrazolium bromide), cytochrome C and 5-bromo-2′-deoxyuridine were obtained from Sigma–Aldrich. The HepG2 and 143B cell lines were obtained from the American Type Culture Collection (ATCC), USA. Fetal Bovine Serum (FBS; 10%) was purchased from Cansera, CANADA. HEPE buffer solution (1 M), which contained HEPES (*N*-2-hydroxyethylpiperazine-*N*′-2-ethane sulfonic acid 238 g/L) in water, was purchased from Sigma–Aldrich CANADA. Trypsin-EDTA was purchased from Gibco BRL.

### 2.2. SPIO production

Silanized SPIO nanoparticles were produced as reported previously (Liu et al., 1998). Briefly, maghemite (average particle size ca. 30 nm by transmission electron microscope, surface area 44 $m^2/g$) was dried in a vacuum oven at reduced pressure and 120 °C for 24 h prior to coating. Tetraethoxysilane (TEOS) distilled in quartz, reagent grade ammonium hydroxide and absolute ethanol distilled in-house, were mixed with the maghemite. The coating reaction was allowed to proceed for 5 h to ensure maximum hydrolysis of TEOS and the formation of the monosilicic acid necessary for condensation. The particles treated as such were separated from solution by a hand-magnet, rinsed with ethanol, dried in a vacuum oven at 110 °C and stored in a desiccator.

### 2.3. Amino-functionalized SPIO (ASPIO)

A literature procedure (Wu and Xu, 2005) was used for surface-amine-functionalization. To effectively hydrolyze the SPIO surfaces, the mesoporous $Fe_3O_4$ particles were steamed for 30 min with boiling deionized water, then recovered and baked at 120 °C to remove free water. The sample was then mixed by vigorous stirring with toluene, followed by slow addition of 3-APTES under continuous mechanical stirring. Reaction under reflux was continued for 4 h. The resulting suspension of amino-SPIOs (ASPIO) nanoparticles was cooled to room temperature and the particles were collected with a hand magnet. After successive washes with toluene, water, and ethanol, the particles were dried in a vacuum oven at room temperature.

### 2.4. ASPIO size measurement

The size distribution of ASPIO was measured using a dynamic light scattering particle size analyzer (BI-90, Brookhaven Instruments Corporation, New York, USA). A few measurements, for comparative purposes, were made using a Beckman Coulter particle analyzer. To reduce the dust contamination, distilled water was filtered through a 0.45 nm membrane filter, then 1 mL was transferred to a quartz cuvette. One drop of the nanoparticle suspension was added to the cuvette and the contents were mixed by gentle shaking, followed by measurement at 20–25 °C. Measured values are given as mean volume-average; dispersion about the mean value is described as the full-width half maximum in square brackets [FWHM]; both values are given in nanometers.

### 2.5. ASPIO surface charge

Zeta potentials were measured using a Zetaphoremeter III (SEPHY/CAD; Laval Lab Inc., France) fitted with a rectangular cell, two hydrogenated palladium electrodes, laser-illumination device and digital camera. SPIO suspensions (~50 mL) were introduced into the electrophoresis cell, and the movement of particles at the stationary layer in the cell was tracked 5 times for each direction by alternating positive/negative electrode potential, at 22 ± 0.1 °C. Software-based image analysis provided the zeta potential value along with other information such as mobility, conductivity and concentration of suspensions.

### 2.6. ASPIO lactosylation (Gal-ASPIO)

ASPIO (~250 mg in colloidal suspension) was mixed with a solution of lactose (1 mM) in water (3 mL), further mixed with a solution of sodium cyanoborohydride (5 mM) in water (3 mL), and then allowed to stand for 7 days, with gentle shaking 3 or 4 times daily. After this derivitization process, the Gal-ASPIO particles were settled by placing the vial onto a small permanent magnet. The aqueous layer was removed by pipette. To remove any free lactose remaining in the sediment, the sediment was washed by briefly shaking with water (5 mL), settling over a magnet and then carefully decanting the water. This washing procedure was repeated five times with water, then three times with 1:1 water/methanol, and finally twice with methanol. Then methanol (4.5 mL) containing acetic anhydride (0.5 mL) was added to the particles and the mixture shaken (3 h) to chemically cap (acetylate) any remaining

non-lactosylated (free) amino residues. Finally the particles were washed in reverse order of the previous cycle and diluted with 5 mL water.

### 2.7. ASPIO acetylation (NAc-ASPIO)

Neutral (amino-capped) particles were prepared by adding ASPIO (250 mg) in colloidal suspension to methanol (4.5 mL) containing acetic anhydride (0.5 mL). This mixture was shaken for 3 h, washed as described above, and then stored in water (5 mL).

### 2.8. Gal-ASPIO assay for galactose content

Galactose, the terminal monosaccharide moiety of lactose, was determined by the phenol/sulfuric acid method (Dubois et al., 1956). Briefly, galactose standard solutions (0 μL, 40 μL, 60 μL, 80 μL, 100 μL, 120 μL; 1 mg/mL; volumetrically diluted to 2 mL), Gal-ASPIO (50 mg/mL; 2 mL) and NAcASPIO (50 mg/mL; 2 mL) were prepared. Phenol reagent (5% in water; 1 mL) and concentrated sulfuric acid (4 mL) were added to each tube, the tubes were sealed and mixed for 1 min, allowed to stand (15 min) at room temperature, then settled over a magnet. The absorbance of each of the standards and samples was measured (490 nm) and the content of the beads was interpolated from a standard curve prepared in this manner.

### 2.9. In vitro cytotoxicity of Gal-ASPIO

HepG2 human hepatoma cells were used to determine the cytotoxicity of Gal-ASPIO in cell culture using the MTT assay (Mosmann, 1983). Briefly, HepG2 cells suspended in Eagle's Minimum Essential Medium (EMEM) supplemented with 10% fetal bovine serum were diluted to $8 \times 10^3$ cells/mL and then plated in 100 μL volumes into 96-well microplates. The cells were incubated (24 h; 37 °C) in air containing 5% $CO_2$. Aliquots (100 μL) of Gal-ASPIO (3 mg/mL; 300 μg/mL, 30 μg/mL, 3 μg/mL; 0.3 μg/mL and 0.03 μg/mL) were added to 10 wells containing HepG2 cells. As a control, EMEM (100 μL) was added in place of cells in 10 wells, and as a background control, EMEM (100 μL) was plated in wells without cells. The plates were incubated (5 days; 37 °C; humidified 95% air and 5% $CO_2$), then dilute 3-(4,5-dimethylthiazol-2-yl)-2,5-diphenyltetrazolium bromide (MTT) solution (50 μL) was added to each well. The plates were incubated (37 °C; 4 h), and then the medium was aspirated, leaving about 20 μL of medium in each well. DMSO (150 μL) was then added to each well, the plates were shaken (15 min) to dissolve the formazan crystals formed, and were then read immediately at 540 nm on an ELISA reader. The percent viability of cells was calculated for each group (Gal-ASPIO, cell control, background control), so that for each MTT assay, the control HepG2 cell viability was 100% by definition.

### 2.10. Cellular binding of Gal-ASPIO and NAc-ASPIO

HepG2 cells ($0.3–0.5 \times 10^6$ cells/dish) were seeded in tissue culture dishes (35 mm plastic) for 2, 3 and 5 days prior to assay. At the time of assay, pre-warmed PBS (1 mL) was used to wash each dish (2×). Gal-ASPIO (or NAc-ASPIO) (200 μL per dish) and pre-warmed EMEM (1 mL) were dispersed evenly within each dish. The dishes were incubated (37 °C; 2 h), washed once with PBS, and then EMEM (1 mL) was added to each dish for a second cycle of incubation (37 °C; 24 h) and washing with PBS (3× 1 mL). Aqueous ethanol (500 μL; 70%, v/v) was added to each dish as the fix solution. After standing at room temperature for 10 min, each dish was washed with PBS (3× 1 mL), and then kept in PBS. The cells were viewed under a phase contrast microscope (ECLIPSE, TS100, Nikon, Japan) and pictures were recorded at 40×, 100×, 200× and 400× magnifications. At the time of assay, the cells were near confluence ($1–1.5 \times 10^6$ cells/dish). Similar procedures were followed using human 143B osteosarcoma cells as ASGPR-non-expressing controls.

### 2.11. Gal-ASPIO cell binding challenge study

The experimental conditions were as described above for the uptake of Gal-ASPIO, except that galactose was added to three dishes, to a final concentration of 65 mM, followed by incubation for 30 min, 1 h and 2 h with the Gal-SPIO. Phase contrast photomicrographs were taken at 100× magnification.

The use of human cell lines for this work was approved by the Biosafety Committee, University of Alberta.

## 3. Results

Two batches of ASPIO were prepared. Both batches were sized, and studied to determine Zeta potential, superparamagnetic properties and the effects of storage on size.

### 3.1. ASPIO properties

The two batches of ASPIO prepared for this work were determined to have mean particle sizes (volume-average) of 61 (ASPIO-61) and 127 (ASPIO-127) nm as determined using the BI-90 method. After storage for 1 year, the mean volume-average particle size increased to 86 nm and 141 nm, respectively. When measured with a BI-90 instrument, the size distribution of ASPIO-61 particles was 10% <37 nm; 25% <46 nm; 50% <58 nm; 75% <72 nm and 90% <89 nm (Fig. 1); measurement using the Beckman Coulter instrument provided a slightly larger average size of 69 nm (Fig. 1, inset). One year later, the ASPIO-61 size had increased to a mean of 86 nm distributed with 10% <48 nm; 25% <61 nm; 50% <80 nm; 75% <104 nm and 90% <131 nm (BI-90 instrument). The ASPIO-127 particles had the following size distribution about the mean: 10% <63 nm; 25% <83 nm; 50% <114 nm; 75% <156 nm and 90% <207 nm, and 1 year later, a mean of 141 nm, with 10% <70 nm; 25% <93 nm; 50% <127 nm; 75% <173 nm and 90% <229 nm.

The electrostatic charges (zeta potential) of ASPIO-61 (Fig. 2) and ASPIO-127 particles (mobility diagram not shown), calculated from the electrophoretic mobility diagrams, were $-43.9 \pm 1.7$ mV and $-38.5 \pm 5.2$ mV, respectively.

Fig. 3 depicts ASPIO-61 magnetization as a function of the applied magnetic field. This typical curve shows that ASPIOs can be

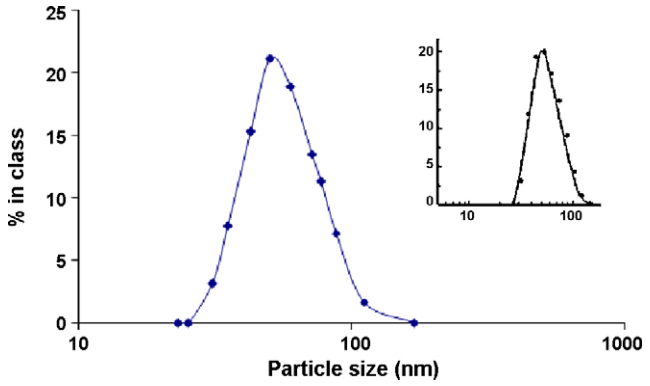


**Fig. 1.** ASPIO-61 particle size distributions (mean 61 nm) as determined using the BI-90 (Brookhaven Instruments Corp.) dynamic light scattering particle size analyzer and (inset) Beckman Coulter particle analyzer (mean diameter 69.6 nm; 82% <88 nm).

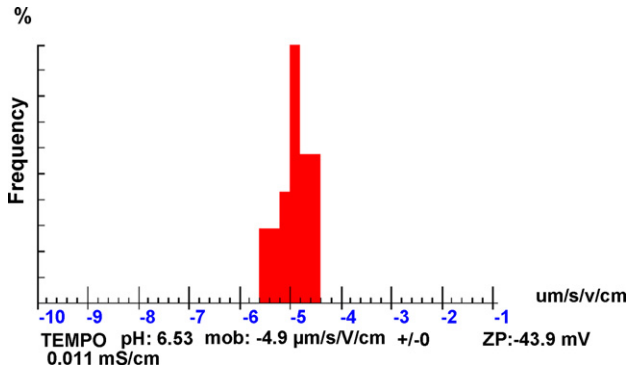


**Fig. 2.** Mobility diagram of ASPIO-61 particles as determined using a Zetaphoremeter III.

highly magnetized in a reversible fashion, i.e. they are superparamagnetic. The saturation magnetization of the ASPIO was found to lie between the values for magnetite ($Fe_3O_4$: 80 emu/g) and maghemite (r-$Fe_2O_3$: 52.7 emu/g) (Wu et al., 2004).

### 3.2. Gal-ASPIO production

Galactose coupling to ASPIO was based on a two-phase reaction starting with lactose, a glucosyl-galactose disaccharide. In order to achieve a reasonably uniform particle size distribution, the ASPIO-lactose mixture was well-stirred before adding $NaBH_3CN$. Addition of $NaBH_3CN$ results in Schiff base formation between the aldehyde group of the ring-open form of the glucose moiety in lactose and

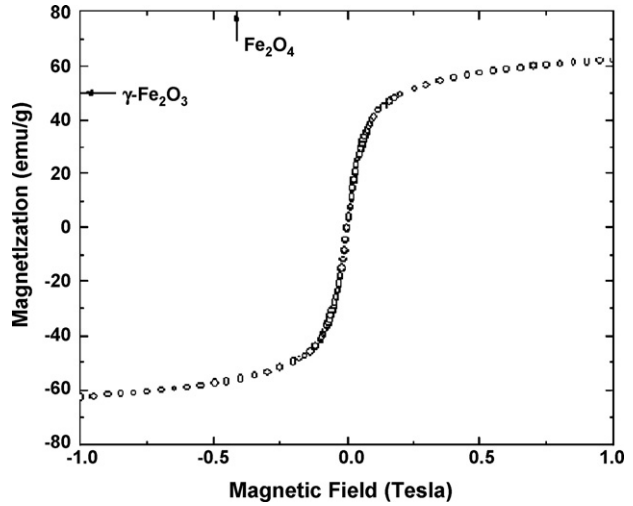


**Fig. 3.** Superparamagnetic property of ASPIO-61 particles measured with a vibrating sample magnetometer (VSM) (Quantum design 9T-PPMS DC Magnetometer/AC Susceptometer, San Diego, CA, USA).

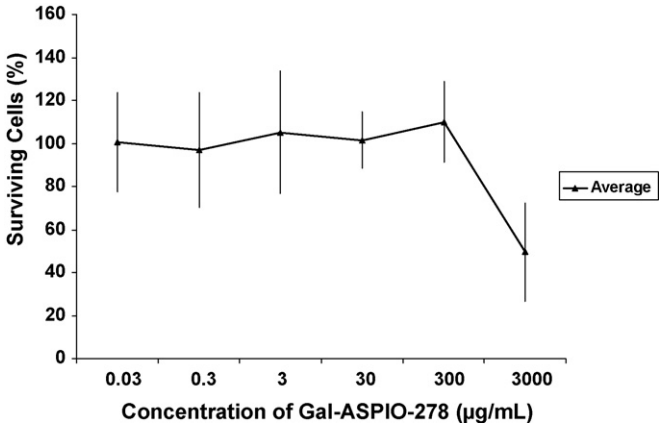


**Fig. 4.** Cytotoxicity of Gal-ASPIO-278 to HepG2 cells in vitro following a 5-day period of incubation. Cell survival was estimated using the MTT cell viability assay (Mosmann, 1983). Data points are mean values with error bars representing standard deviations, $n = 10$.

the ASPIO amino groups. Two different sizes of galactose-terminal ASPIO were prepared. As shown in Table 1, galactose-derivitization substantially increased the mean volume-average size of the ASPIO. Neutral (acetylated) NAc-ASPIO particles (controls) were made using a standard *N*-acetylation technique. ASPIO-61 were used to prepare NAc-ASPIO-302 and Gal-ASPIO-278, and ASPIO-127 to were used to prepare NAc-ASPIO-326 and Gal-ASPIO-337. One month after coating (lactosylation) or capping (acetylation), respectively, the sizes of both groups appeared to have increased marginally (5–10%) but this was not statistically validated. However, these particles began to aggregate upon standing in solution for approximately 3 months (visual observation).

The galactose content of the galactose-terminal ASPIO varied from 0.73 μg to 0.95 μg of galactose per mg (36.3–47.7 μg/mL). Loss of the galactosyl moieties was found minimal over the period of 1 month (Table 2).

Gal-ASPIO-278 cytotoxicity ($LC_{50}$) for HepG2 cells, as determined by MTT cell survival assay, was approximately 1500 μg/mL, with no measurable toxicity observed below 150 μg/mL (Fig. 4).

Gal-ASPIO-278 uptake by HepG2 cells in culture was determined using phase contrast microscopy over 5 days of culture (at days 2, 3, 5), at magnifications of 40×, 100×, 200× (Fig. 5) and 400×. Although no quantification was attempted, the association of Gal-SPIO-278 with HepG2 cells was visibly greater than that of NAc-ASPIO-302; no association was observed with 143B cells was observed for either NAc-ASPIO-302 or Gal-ASPIO-278, and HepG2 cells did not show any affinity for NAc-ASPIO-302. Qualitative examination of the photomicrographs showed that uptake of Gal-ASPIO-278 by HepG2 cells was diminished in the presence of galactose as a competing agent (Fig. 6).

**Table 1**
Mean volume-average sizes of ASPIOs, NAc-ASPIOs and Gal-ASPIOs, in nm [FWHM], as determined by BI-90 (Brookhaven Instruments Corp.) dynamic light scattering scanning particle sizer

| ASPIO source batch | ASPIO volume-average (nm) [FWHM] | ASPIO volume-average (nm) [FWHM][a] | NAc-ASPIO volume-average (nm) [FWHM] | Gal-ASPIO volume-average (nm) [FWHM] |
|---|---|---|---|---|
| ASPIO-61 | 61 [42] | 86 [70] | 302 [280] (314)[b] | 278 [309] (290)[b] |
| ASPIO-127 | 127 [125] | 141 [138] | 326 [308] (376)[b] | 337 [372] (365)[b] |

Full-width at half maximum [FWHM].
[a] Measured after standing for 1 year.
[b] Values in parentheses are mean volume-average size measured 30 days after manufacture.

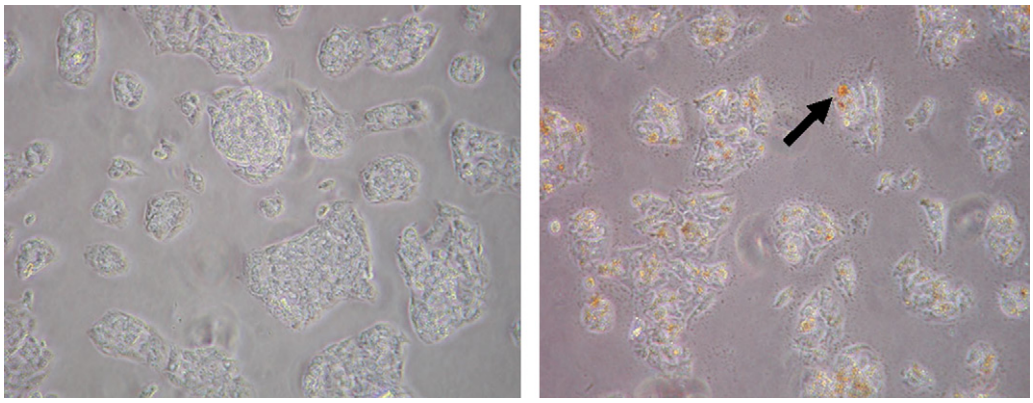

**Fig. 5.** Receptor-mediated association between Gal-ASPIO-278 and HepG2 cells. The image shows HepG2 cells on culture plates in the absence (control; left) and presence of Gal-ASPIO-278 (right). Cells were cultured for 3 days and photomicrographs were taken at 200× magnification. The arrow points out the Gal-ASPIO-278 (yellow-brown spots) associated with a cell. (For interpretation of the references to color in this figure legend, the reader is referred to the web version of the article.)

**Table 2**
Assay for galactose content in Gal-ASPIO (μg/mL)

| Galactose assay | Galactose (μg/mg) | |
|---|---|---|
| | Gal-ASPIO-278 | Gal-ASPIO-337 |
| Fresh | 0.95 ± 0.06 | 0.77 ± 0.09 |
| 30 days | 0.80 ± 0.08 | 0.78 ± 0.07 |

## 4. Discussion

The classic phenol/sulphuric acid colorimetric reaction (Dubois et al., 1956) for the determination of galactose residues, in which simple sugars give an orange yellow color, is sensitive and the color is stable when applied to Gal-ASPIO. Measurements confirmed that galactose to ASPIO coupling yields, when using 1 mM lactose per g ASPIO, were consistent from batch to batch.

The two pre-derivitization (ASPIO) batches prepared for this work had initial volume-average particle sizes of 61 nm and 127 nm, and these increased to 86 nm and 141 nm, respectively after storage for 1 year. This increase was not anticipated on the basis of the zeta potential measurements (−43.5 mV and −38.3 mV, respectively, since suspensions having zeta potentials of 30 mV or more are considered to be stable (Hunter, 1981).

Galactose residues of the triantennary oligosaccharide (ASOR) bind simultaneously to the ASGPR binding site, a lattice at the vertices of a triangle with sides of 15 Å, 22 Å, and 25 Å (ASGPR trimer) (Stockert, 1995). For binding, the galactose moiety can be coupled (at C-1) to any number of residues, including sugars. To prepare ASPIOs that feature galactose-terminal functional groups, we coupled lactose (a glucose-galactose disaccharide); i.e., coupling at C-1 of the lactose glucosyl residue to an amino function on the ASPIO surface affords the desired galactose-terminal ASPIO.

Lactose coupling to ASPIO is a two-phase reaction. The lactose solution was first added to a suspension of ASPIO and this was stirred to ensure homogeneity. $NaBH_3CN$ was then added with stirring, resulting in Schiff base formation between the aldehyde group of the open (aldehyde) glucose form of lactose and the amino group of the particles. Optimum conditions for coupling lactose to ASPIO have not yet been established.

Derivatization (i.e., *N*-lactosylation or *N*-acetylation) would be expected to lead to increased aggregation and flocculation because of charge neutralization. Indeed, particle sizes increased by a factor of 2–3 times, for both the neutral (NAc-ASPIO) and the polyhydric (Gal-ASPIO) amino caps. Thus, ASPIO-61 enlarged to NAc-ASPIO-302 after acetylation and to Gal-ASPIO-278 upon lactosylation.

The >50 nm ASPIO volume-average size is relatively large for biological applications. Reported literature values for derivatized SPIOs range from 4.3–6.0 nm (31 mm with dextran coat; Brillet et al., 2005) to 8 nm (24 nm with *meso*-2,3-dimercaptosuccinic acid coat; Brillet et al., 2005) to 12–14 nm (PEG-phospholipid coat; Nitin et al., 2004) and 10–15 nm (unchanged after conjugation with a monoclonal antibody; Liang et al., 2007). In other cases, however, substantial enlargement upon derivitization, even of small particles, has been reported. For example, 10–14 nm particles expanded to 90–100 nm when derivatized with Protein G and Annexin V (Smith et al., 2007), to 195 nm when formulated in liposomes

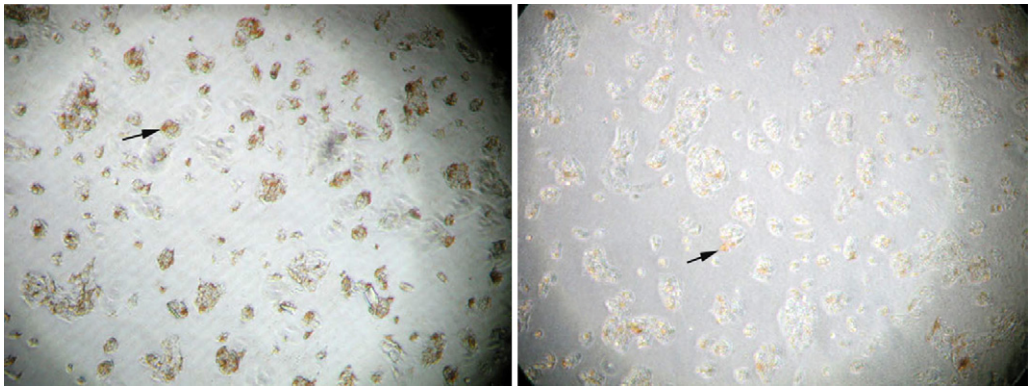

**Fig. 6.** Galactose-mediated competitive inhibition of Gal-ASPIO-278 binding to HepG2 cells in vitro. Cells were incubated for 2 h with Gal-ASPIO-278 alone (left), and Gal-ASPIO-278 and galactose (right). Arrows show site of Gal-ASPIO (yellow-brown spots) associated with cells (white-blue). Photomicrographs were taken at 100× magnification. (For interpretation of the references to color in this figure legend, the reader is referred to the web version of the article.)

(Martina et al., 2005) and to 280 nm when formulated with oleic acid (Okassa et al., 2007). Ferumoxides (dextran coated), ferumoxtran (dextran covered), and ferumoxsil (siloxane coated) SPIO, with mean SPIO crystal diameters (volume weighted distributions) of 4.8–5.6 nm, 5.8–6.2 nm, and 7.9–8.8 nm, respectively, reportedly increased to 50 nm, 30 nm and 300 nm (volume-weighted distribution), respectively, upon coating, as determined from XRD line-broadening (Jung, 1995; Jung and Jacobs, 1995). No rational explanations of these effects have been forthcoming.

Preliminary investigation of the interaction of Gal-ASPIO-278 in cell culture indicated (Fig. 5) that these particles have a strong association with HepG2 cells. This is attributed to affinity of the galactosyl residues to the ASGPR expressed on the surface of HepG2 cells (Li et al., in press). This receptor was not expressed by the control cell line, 143B human osteosarcoma cells, and indeed no Gal-ASPIO binding was observed photomicrographically (not shown). Furthermore, no association was observed for control (NAc-ASPIO-302) particles for either HepG2 or 143B cells, and binding of Gal-ASPIO-278 to HepG2 was reduced in the presence of galactose (Fig. 6). Galactose has been shown to competitively inhibit and dissociate the binding of another galactosylated ligands, ASOR, to HepG2 cells (Li et al., in press), and similar effects now support the model of specific interaction between Gal-ASPIO-278 and ASGPR. The galactose content of both Gal-SPIO-278 and Gal-SPIO-337 (approximately 1 μg per mg of Gal-SPIO) therefore appears to be adequate to promote triantennary binding to ASGPR, thereby anchoring the ligand to the receptor and possibly promoting endocytosis of the Gal-SPIO construct. Unfortunately, the current methodology does not support differentiation between surface binding and internalization (uptake). Direct comparisons to literature data are not possible, since no ASGPR-targeted nanoparticle studies have been reported. However, it is known that small (30 nm), medium (300 nm) and large (3500 nm) non-derivatized SPIO reduce the T2 relaxation times of liver by 50%, 40% and 15%, respectively, and of spleen by 60%, 65%, and 25%, respectively, following intravenous injection at 1 mg Fe/kg into rabbits (Bach-Gansmo et al., 1994), implying proximity to intracellular as well as extracellular water. Smaller, non-targeted particles are reported to be sequestered by phagocytic Kupffer cells in the normal reticuloendothelial system, but are not retained in tumor tissue (Tanimoto and Kuribayashi, 2006; Boutry et al., 2006).

The low cytoxicity ($LD_{50} \sim 1500$ μg/mL) of Gal-ASPIO-278 is in line with cytotoxicity reported for non-derivatized SPIOs to adult mesenchymal stem cells (Schäfer et al., 2007). Unfortunately, these literature data are not directly comparable to the Gal-ASPIO-278 data because that study focused on iron dose, did not exploit any selective transport mechanism, and did not report particle size. The MTT assay used in the Gal-ASPIO-278 study is convenient and simple to use, but high variability and non-specificity mitigate the use of additional histopathological and morphological methods and cytogenetic analysis in future studies.

## 5. Conclusions

Amine-functionalized superparamagnetic iron oxide nanoparticles (ASPIO) have been characterized, and derivatized with lactose to form galactose-terminal (Gal-ASPIO) nanoparticles. Gal-ASPIO-278 have low cytotoxicity ($LD_{50} \sim 1500$ μg/mL) despite substantial, receptor-mediated association with HepG2 cells. Neutral NAc-SPIO-302 are not taken up by HepG2 cells, and Gal-ASPIO-278 are not taken up by cells not expressing ASGPR, establishing a firm link between the ASGPR endocytosis mechanism of uptake and galactose presentation by Gal-ASPIO-278.

## References


Bach-Gansmo, T., Fahlvik, A.K., Ericsson, A., Hemmingsson, A., 1994. Superparamagnetic iron oxide for liver imaging. Comparison among three different preparations. Invest. Radiol. 29, 339–344.

Boutry, S., Laurent, S., Elst, L.V., Muller, R.N., 2006. Specific E-selectin targeting with a superparamagnetic MRI contrast agent. Contrast Media Mol. Imaging 1, 15–22.

Brillet, P.Y., Gazeau, F., Luciani, A., Bessoud, B., Cuénod, C.A., Siauve, N., Pons, J.N., Poupon, J., Clément, O., 2005. Evaluation of tumoral enhancement by superparamagnetic iron oxide particles: comparative studies with ferumoxtran and anionic iron oxide nanoparticles. Eur. Radiol. 15, 1369–1377.

Bulte, J.W., Kraitchman, D.L., 2004. Iron oxide MR contrast agents for molecular and cellular imaging. NMR Biomed. 17, 484–499.

Corot, C., Robert, P., Idée, J.M., Port, M., 2006. Recent advances in iron oxide nanocrystal technology for medical imaging. Adv. Drug Deliv. Rev. 58, 1471–1504.

Dubois, M., Gilles, K.A., Hamilton, J.K., Rebers, P.A., Smith, F., 1956. Colorimetric method for determination of sugars and related substances. Anal. Chem. 28, 350–356.

Hamoudeh, M., Fessi, H., 2006. Preparation, characterization and surface study of poly-epsilon caprolactone magnetic microparticles. J. Colloid Interf. Sci. 300, 584–590.

Hunter, R.J., 1981. Zeta-Potential in Colloid Science. Academic Press, London.

Josephson, L., Tung, C.-H., Moore, A., Weissleder, R., 1999. High-efficiency intracellular magnetic labeling with novel superparamagnetic-Tat peptide conjugates. Bioconjug. Chem. 10, 186–191.

Jung, C.W., 1995. Surface properties of superparamagnetic iron oxide MR contrast agents: ferumoxides, ferumoxtran, ferumoxsil. Magn. Reson. Imaging 13, 675–691.

Jung, C.W., Jacobs, P., 1995. Physical and chemical properties of superparamagnetic iron oxide MR contrast agents: ferumoxides, ferumoxtran, ferumoxsil. Magn. Reson. Imaging 13, 661–674.

Kim, K.S., Lei, Y., Stolz, D.B., Liu, D., 2007. Bifunctional compounds for targeted hepatic gene delivery. Gene Ther. 14, 704–708.

Li, Y., Huang, G., Diakur, J., Wiebe, L.I., in press. Targeted delivery of macromolecular drugs: asialoglycoprotein receptor (ASGPR) expression by selected hepatoma cell lines used in antiviral drug development. Curr. Drug Deliv.

Li, Y., Xu, X., Deng, C., Yang, P., Zhang, X., 2007. Immobilization of trypsin on superparamagnetic nanoparticles for rapid and effective proteolysis. J. Proteome Res. 6, 3849–3855.

Liang, S., Wang, Y., Yu, J., Zhang, C., Xia, J., Yin, D., 2007. Surface modified superparamagnetic iron oxide nanoparticles: as a new carrier for bio-magnetically targeted therapy. J. Mater. Sci. Mater. Med. 18, 2297–2302.

Liu, Q., Xu, Z., Finch, J.A., Egertan, R., 1998. A novel two-step silica coating process for engineering magnetic nanocomposites. Chem. Mater. 10, 3936–3940.

Martina, M.S., Fortin, J.P., Ménager, C., Clément, O., Barratt, G., Grabielle-Madelmont, C., Gazeau, F., Cabuil, V., Lesieur, S., 2005. Generation of superparamagnetic liposomes revealed as highly efficient MRI contrast agents for in vivo imaging. J. Am. Chem. Soc. 127, 10676–10685.

Mohapatra, S., Pramanik, N., Ghosh, S.K., Pramanik, P., 2006. Synthesis and characterization of ultrafine poly(vinylalcohol phosphate) coated magnetite nanoparticles. J. Nanosci. Nanotechnol. 6, 823–829.

Morell, A.G., Irvine, R.A., Sternlieb, I., Scheinberg, I.H., Ashwell, G., 1968. Physical and chemical studies on Ceruloplasmin. V. Metabolic studies on sialic acid-free ceruloplasmin in vivo. J. Biol. Chem. 243, 155–159.

Mosmann, T., 1983. Rapid colorimetric assay for cellular growth and survival: application to proliferation and cytotoxicity assays. J. Immunol. Methods 65, 55–63.

Nitin, N., LaConte, L.E., Zurkiya, O., Hu, X., Bao, G., 2004. Functionalization and peptide-based delivery of magnetic nanoparticles as an intracellular MRI contrast agent. J. Biol. Inorg. Chem. 9, 706–712.

Okassa, L.N., Marchais, H., Douziech-Eyrolles, L., Hervé, K., Cohen-Jonathan, S., Munnier, E., Soucé, M., Linassier, C., Dubois, P., Chourpa, I., 2007. Optimization of iron oxide nanoparticles encapsulation within poly(D,L-lactide-*co*-glycolide) sub-micron particles. Eur. J. Pharm. Biopharm. 67, 31–38.

Palmacci, S., Josephson, L., 1993. Synthesis of polysaccharide covered superparamagnetic oxide colloids. US Patent 5,262,176.

Schäfer, R., Kehlbach, R., Wiskirchen, J., Bantleon, R., Pintaske, J., Brehm, B., Gerbe, A., Wolburg, H., Claussen, C., Northoff, H., 2007. Transferrin receptor upregulation: in vitro labeling of rat mesenchymal stem cells with superparamagnetic iron oxide. Radiology 244, 514–523.

Shamim, N., Hong, L., Hidajat, K., Uddin, M.S., 2007. Thermosensitive polymer (*N*-isopropylacrylamide) coated nanomagnetic particles: preparation and characterization. Colloids Surf. Biointerf. 55, 51–58.

Silva, A.K., Silva, E.L., Carrico, A.S., Egito, E.S.T., 2007a. Magnetic carriers: a promising device for targeting drugs into the human body. Curr. Pharm. Res. 13, 1179–1185.

Silva, A.K., da Silva, E.L., Oliveira, E.E., Nagashima, T., Soares, L.A., Medeiros, A.C., Araujo, J.H., Araujo, I.B., Carrico, A.S., Egito, E.S.T., 2007b. Synthesis and characterization of xylan-coated magnetite microparticles. Int. J. Pharm. 334, 42–47.

Smith, B.R., Heverhagen, J., Knopp, M., Schmalbrock, P., Shapiro, J., Shiomi, M., Moldovan, N.I., Ferrari, M., Lee, S.C., 2007. Localization to atherosclerotic plaque and biodistribution of biochemically derivatized superparamagnetic iron oxide nanoparticles (spions) contrast particles for magnetic resonance imaging (MRI). Biomed. Microdevices 9, 719–727.

Stockert, R.J., 1995. The asialoglycoprotein receptor: relationships between structure, function, and expression. Physiol. Rev. 75, 591–609.

Tanimoto, A., Kuribayashi, S., 2006. Application of superparamagnetic iron oxide to imaging of hepatocellular carcinoma. Eur. J. Radiol. 58, 200–216.
Wagner, S., Schnorr, J., Pilgrimm, H., Hamm, B., Taupitz, M., 2002. Monomer-coated very small superparamagnetic iron oxide particles as contrast medium for magnetic resonance imaging: preclinical in vivo characterization. Invest. Radiol. 37, 167–177.
Wu, P., Xu, Z., 2005. Silanation of nanostructured mesoporous magnetic particles for heavy metal recovery. Ind. End. Chem. Res. 44, 816–824.
Wu, J., Nantz, M.H., Zern, M.A., 2002. Targeting hepatocytes for drug and gene delivery: emerging novel approaches and applications. Proc. Front. Biosci. 7, 717–725.
Wu, P., Zhu, J., Xu, Z., 2004. Template-assisted synthesis of mesoporous magnetic nanocomposite particles. Adv. Funct. Mater. 14, 345–351.
Zhang, C., Wängler, B., Morgenstern, B., Zentgraf, H., Eisenhut, M., Untenecker, H., Krüger, R., Huss, R., Seliger, C., Semmler, W., Kiessling, F., 2007. Silica- and alkoxysilane-coated ultrasmall superparamagnetic iron oxide particles: a promising tool to label cells for magnetic resonance imaging. Langmuir 23, 1427–1434.
Zhao, M., Kircher, M.F., Josephson, L., Weissleder, R., 2002. Differential conjugation of tat peptide to superparamagnetic nanoparticles and its effect on cellular uptake. Bioconjug. Chem. 13, 840–844.